

SEVENTEENTH EUROPEAN ROTORCRAFT FORUM

Paper No. 91 - 26

A SIMULATION STUDY OF TILTROTOR VERTICAL  
TAKEOFF PROCEDURES USING CONVENTIONAL  
AND VARIABLE DIAMETER ROTOR SYSTEMS

M. POLLACK, F. WARBURTON

SIKORSKY AIRCRAFT  
STRATFORD, CONNECTICUT

H. C. CURTISS

PRINCETON UNIVERSITY  
PRINCETON, NJ

September 24 - 26, 1991

Berlin, Germany

Deutsche Gesellschaft für Luft- und Raumfahrt e.V. (DGLR)  
Godesberger Allee 70, 5300 Bonn 2, Germany

OPGENOMEN IN  
GEAUTOMATISEERDE  
CATALOCUS

N61296



A SIMULATION STUDY OF TILTROTOR VERTICAL  
TAKEOFF PROCEDURES USING CONVENTIONAL  
AND VARIABLE DIAMETER ROTOR SYSTEMS

M. Pollack, F. Warburton

Sikorsky Aircraft  
Stratford, Connecticut

H. C. Curtiss

Princeton University  
Princeton, NJ

**Abstract**

An interactive real time computer simulation has been developed to study tiltrotor performance and vertical take-off procedures for conventional and variable diameter tiltrotor (VDTR) aircraft designs. Aerodynamic and preliminary design methods were used to define a conventional tiltrotor and five unique VDTR aircraft, primarily intended for commercial application. A test program was conducted with the simulator, emphasizing tiltrotor Category A vertical take-off procedures and performance aspects. This paper introduces the aircraft design specifications, and describes the tiltrotor flight mechanics simulation methodology, computer simulation architecture and graphics features. Results of the simulation study are presented and discussed in detail.

Conclusions of this study indicate that while a variable diameter tiltrotor adds complexity and weight to the rotor system relative to a conventional design, significant benefits can be realized with a VDTR design. These benefits include improvements in Category A performance, climb capability, powerplant efficiency, and acoustic levels. The source for some of these improvements is manifested in the characteristics of low disk loading rotors that operate in close lateral proximity to each other in helicopter mode. An improved balance between cruise and contingency power requirements can also be achieved with a VDTR aircraft, enhancing performance and cost considerations associated with powerplant selection. These findings support the VDTR concept and warrant further analyses of VDTR and conventional tiltrotors.

## 1. Introduction

Recent studies (References 1,2) indicate that the civil tiltrotor concept is technically and economically feasible. For the tiltrotor to achieve success in the commercial market it must be safe, reliable, capable of all-weather operation and economically competitive. As the tiltrotor concept works to gain acceptance as viable mode of air travel, it is imperative that the research be performed to advance technology and identify optimum design configurations that can effectively move into the market when it is ready. Tiltrotor research has been ongoing at Sikorsky Aircraft. Reference 3 introduces the technology that makes a variable diameter rotor system a candidate for tiltrotor application. Conventional tiltrotor aircraft designs typically possess various compromises associated with its aerodynamic features. For the rotor these compromises include blade twist and planform designs that result in performance penalties relative to designs that are optimized for either hover or cruise. The conventional tiltrotor typically retains the undesirable attributes of a high rotor disk loading in hover and an oversized propeller in cruise. Cruise efficiency is often improved by reducing RPM. A variable diameter tiltrotor (VDTR) has the appealing benefits associated with low hover disk loading and a properly sized propeller that yields an increased propeller efficiency without significant RPM reduction. Several other significant advantages also exist and will be discussed for the VDTR concept. Of course, there are disadvantages associated with the VDTR in the form of increased complexity, reduced rotor hover Figure of Merit and increased rotor weight. While trade studies are required for any rotor design development, the details of the aerodynamic trades considered for each rotor system design is outside the scope of this work. Rather, two existing rotor designs, one conventional and the other variable diameter, that have undergone some optimization for tiltrotor application, are used with preliminary design methods to define aircraft configurations that are analyzed by an interactive, real time simulation program that has been developed specifically for this purpose. In total, six configurations have been analyzed, one conventional tiltrotor and five unique VDTRs.

This simulation development was initiated in 1988 with the objective of providing a tiltrotor model for Sikorsky Aircraft's real time workstation simulator. A non-linear real-time model of a tiltrotor aircraft with six rigid body degrees of freedom was developed which includes detailed treatment of the rotor and wing forces acting on the aircraft. The rotor wake/wing interaction is estimated consistent with published V-22 flight data (Reference 4), and the wing aerodynamics are described through the full angle of attack range from  $-90^\circ$  to  $+90^\circ$ . Power required is modelled in considerable detail. Interference effects between the lifting rotors which can be used to considerable advantage in the variable diameter concept are also included. The pitch, roll, and yaw moments are modelled in terms of the important flying qualities parameters such as the control sensitivities, angular damping derivatives, and directional stability. These quantities are input parameters, and are currently representative of the V-22. The model is flown by a simulation pilot in real time to generate many of the results presented in this paper. Controls include collective and cyclic pitch, elevator and rudder deflection, nacelle tilt, and flap deflection. To facilitate interactive control, the simulation incorporates an inside-out, or cockpit perspective. Rotor speed, rotor radius, and flap deflection may be programmed as a function of aircraft geometry or flight condition during a flight. To accurately simulate Category A takeoff profiles a rotor speed degree of freedom can be included.

The material that is contained within includes a description of the configurations analyzed, a summary of the flight mechanics methodology in the simulation, results from the interactive simulation runs, and conclusions based on the results.

## 2. Aircraft Preliminary Design Specifications

Each of six aircraft designs satisfy an identical civil transport mission. The mission assumed payload consisting of 30 passengers plus flight crew, a range of 600 nautical miles, a takeoff altitude of approximately 1650 feet with a temperature of ISA + 10°C, a cruise altitude of about 25000 feet and a cruise speed of 300 knots. Preliminary design methodology is based on consistent technology levels that incorporate extensive use of composite structures and fly by wire controls. Table 1 presents design specifications for the six aircraft in a non-dimensional format, where (parameter)<sub>b</sub> refers to the Baseline quantity for a particular parameter.

Table 1 Nondimensional Tiltrotor Aircraft Preliminary Design Specifications

Design	Baseline	VDTR-1	VDTR-2	VDTR-3	VDTR-4	VDTR-6
Disk loading, psf	14.2	14.2	14.2	10.0	10.0	10.0
Max Cont Pwr/(MCP) <sub>b</sub> , sls	1.0(A)	1.0	.974(A)	1.0	.874(cr)	.871(cr)
(OEI, 30 sec Pwr)/MCP, sls	1.213	1.213	1.213	1.213	1.213	1.213
Nacelle spacing/Radius	2.62	2.054	2.054	2.044	2.044	1.931
TakeOff GW/(TOGW) <sub>b</sub>	1.0	.999	.996	1.067	1.048	1.026
Empty Wt/(EW) <sub>b</sub>	1.0	1.007	1.003	1.107	1.083	1.067
Fuel/(Fuel) <sub>b</sub>	1.0	.964	.959	.993	.963	.878
Payload/(Payload) <sub>b</sub>	1.0	1.0	1.0	1.0	1.0	1.0
(EW/GW)/(EW/GW) <sub>b</sub>	1.0	1.008	1.007	1.037	1.034	1.040
(XMSN Rating)/(XMSN) <sub>b</sub>	1.0	1.052	1.048	.927	.910	.908
Diameter/(Diameter) <sub>b</sub> , hover	1.0	.999	.995	1.228	1.217	1.205
Cruise/Hover Diameter	1.0	.66	.66	.66	.66	.66
(Hover ΩR)/(Hover ΩR) <sub>b</sub>	1.0	1.0	1.0	1.0	1.0	1.0
(Cruise ΩR)/(Hover ΩR) <sub>b</sub>	.80	.627	.627	.627	.627	.627
Solidity/(Solidity) <sub>b</sub> , hover	1.0	1.0	1.0	.71	.71	.705
Number of Blades	4	4	4	3	3	3
Rotor/Fuselage Clearance, ft	2.6	3.9	3.8	5.1	5.0	2.0
Wing Span/(Span) <sub>b</sub>	1.0	1.09	1.09	1.34	1.32	1.26
Wing Area/(Wing Area) <sub>b</sub>	1.0	1.08	1.07	1.28	1.27	1.20
Aspect Ratio	6.1	6.76	6.75	8.52	8.45	8.07
Wing Airfoil t/c	.21	.21	.21	.21	.21	.21
Drag Area/(Drag Area) <sub>b</sub>	1.0	1.0	1.0	1.05	1.04	1.02
Flap Chord/Wing Chord	.30	.30	.30	.30	.30	.30
Vertical Drag/Thrust	.080	.080	.080	.066	.066	.072
Rotor Figure of Merit	.80	.76	.76	.76	.76	.76
Cruise Propulsive Eff.	.83	.86	.86	.86	.86	.86

(cr) Engine sized by cruise

(A) Engine sized by Category A OEI takeoff

Some of the numerous design variations between configurations are dictated by other design features. These parameters are disk loading, powerplant, rotor system and nacelle spacing, and are listed first in Table 1. The Baseline configuration has a conventional rotor with a 14.2 pounds per square foot (psf) disk loading (relatively high compared to a helicopter), a powerplant that is sized by Category A One Engine Inoperative (OEI) takeoff requirements, and nacelle spacing that is determined by desired rotor/fuselage clearance. The VDTR designs feature variable diameter rotors, of course. VDTR powerplants are chosen to be the same as that of the Baseline for odd numbered configurations (nos. 1,3). Even numbered configuration (nos. 2, 4, 6) powerplants are varied (or rubberized), and sized by

either Category A or cruise requirements. Disk loadings are chosen as 14.2 psf for the VDTR-1 and VDTR-2, equal to the Baseline. A disk loading of 10.0 psf, more typical of a helicopter, is assumed for the VDTR-3, -4, -6. Nacelle spacing is either chosen such that rotor disks have a 1 foot clearance between edges of adjacent rotor disks (VDTR-1 thru -4); or nacelle spacing is chosen such that rotor disks will overlap by some specified amount (VDTR-6). A design with fixed Baseline engines, low disk loading and overlapped rotors would have been designated VDTR-5, but this was not analyzed. Instead, the VDTR-6 was chosen in an attempt to maximize the benefit available from the side by side rotor interference. That is, rotors that operate in close lateral proximity to each other, or in a side by side configuration, benefit from an interference upwash induced by the other rotor. This topic will be expanded later. Table 2 presents the matrix of VDTR designs, highlighting the primary design parameters discussed above.

**Table 2 VDTR Aircraft Primary Design Parameter Variation**

	VDTR-1	VDTR-2	VDTR-3	VDTR-4	VDTR-5*	VDTR-6
<b>Disk Loading, psf</b>	BL	BL	10.0	10.0	10.0	10.0
<b>Engine</b>	BL	Rubber	BL	Rubber	BL	Rubber
<b>Disk/Disk Spacing, feet</b>	1.0	1.0	1.0	1.0	-1.73	-1.73

BL - same value as Baseline, see Table 1

\* - not analyzed

Several additional design features should be noted in Table 1. VDTR rotor diameter retracts by way of a jackscrew mechanisms (Reference 3) that is concealed within an elliptical, telescoping spar. The retracted diameter is 66% of the extended diameter in hover. This results in higher propulsive efficiencies in airplane mode and accounts for some of the VDTR fuel saving capability. Peak propulsive efficiency is obtained by reducing VDTR RPM by only 5%, as opposed to a 20% RPM reduction required by the Baseline. For the VDTR, this small RPM reduction enhances powerplant performance over the entire operating range relative to the Baseline. These engine advantages are itemized below and are discussed at length in Reference 5.

1. For a typical turboshaft engine, as RPM is reduced from the 100% design point, power turbine efficiency and compressor efficiency decreases while SFC increases. The VDTR designs, which undergo a 5% RPM reduction in cruise, will not absorb as large a penalty as is imposed by the 20% RPM reduction for the Baseline.
2. Engine dry mass in Table 2-1 for the VDTR-4 and VDTR-6 is nearly 10% less than that of the Baseline. This can reduce total operating costs by about 0.9% according to Reference 5.
3. The VDTR-4 and VDTR-6 engine price should be reduced relative to the Baseline. Not only does the reduced power requirement directly affect price, but the minor RPM variations associated with the VDTR designs allows installation of a modern (perhaps existing) turboshaft engine. This would avoid cost increases associated with specialized engine development aimed at optimizing power turbine and compressor efficiencies for significant RPM variations.
4. Engine dimensions will be smaller, reducing aircraft drag by a small amount.

5. The VDTR-4 and VDTR-6 engines provide a significantly more balanced design than the Baseline. The VDTR rubber engines are sized by cruise requirements, making available a slight excess of welcome OEI power that enhances operation at altitudes and temperatures that are higher and hotter than the design condition.

Internal cabin noise that propagates from the rotor/prop blades should be less for the VDTR than it is for the Baseline. This results from diameter retraction. VDTR rotational tip speed is 22% lower than the Baseline tip speed in cruise. Also, blade tip/fuselage clearance is greater for the VDTR designs that do not have overlapping rotors in helicopter mode.

Transmissions are sized 15% greater than each aircraft's hover out of ground effect (HOGE) power. Since transmission torque limits are constant with RPM, the VDTR transmission rating will be reduced by only 5% in airplane mode relative to the 20% reduction for the Baseline. This clearly provides more climb power in airplane mode than is available to the Baseline. This topic is discussed more thoroughly in the results section.

The high root cutout of the VDTR, required for diameter reduction, degrades hover Figure of Merit. This .04 decrease in Figure of Merit results from the increased profile power requirements of the exposed elliptical spar, and from the cutout effect on induced efficiency. Despite this fact, low disk loading VDTR designs have lower total hover powers than the Baseline, as will be discussed.

The VDTR is also penalized by a 23% increase in rotor system weight. This is due to the associated VDTR hardware, relative to a Baseline rotor designed for the equivalent tip speed, solidity and radius as an extended diameter VDTR. The weight penalty, however, is offset by a number of other factors. A significant weight savings results from the ability to move the nacelles inboard so that the extended rotor disks are within one foot of each other. In order to react a tiltrotor's hover bending moments and provide adequate stiffness in cruise, the Baseline wing structure is significantly heavier per unit span than a normal wing. Reduced nacelle spacing decreases area and weight of the main wing component. Secondly, shorter wing span reduces the bending and torsional arms thus enabling the same natural wing frequencies with a lighter wing structure. Lastly, wing tip extensions can be added to decrease induced drag and save fuel. These extensions protrude only to the hover root cutout position, minimizing additional vertical drag penalties in hover. The tip area incurs little additional weight.

### 3. Simulation Flight Mechanics Methodology

#### 3.a Wing and Fuselage Aerodynamics

Wing aerodynamics are modelled over the angle attack range of  $-90^\circ$  to  $+90^\circ$  assuming that the lift and drag coefficients can be analytically represented by simple functions in three regions; pre-stall, the lift coefficient is a linear function of angle of attack; stall, the lift coefficient is constant; and post-stall, the resultant wing force coefficient is assumed normal to the chord, and varies appropriately to model experimental results available near  $-90^\circ$ . Wing angle of attack computation includes the effect of rotor downwash. The airfoil section is a NACA 43021 (Reference 6) with a 30 percent chord plain flap. Experimental data from References 7 and 8 are used to model the effects of flap deflection on the wing aerodynamic characteristics. A flap deflection schedule as a function of airspeed is used to reduce the download at low speeds, and increase the lift with increasing airspeed without a large profile drag penalty. Figures 1 and 2 show the wing lift and drag coefficients as a function of angle of attack for zero flap deflection and an aspect ratio of 6.1. Fuselage lift and drag characteristics are estimated to be similar to a clean helicopter fuselage (S-76).

Figure 1 Wing Lift Coefficient Representation  
Zero Flap Deflection, AR = 6.1

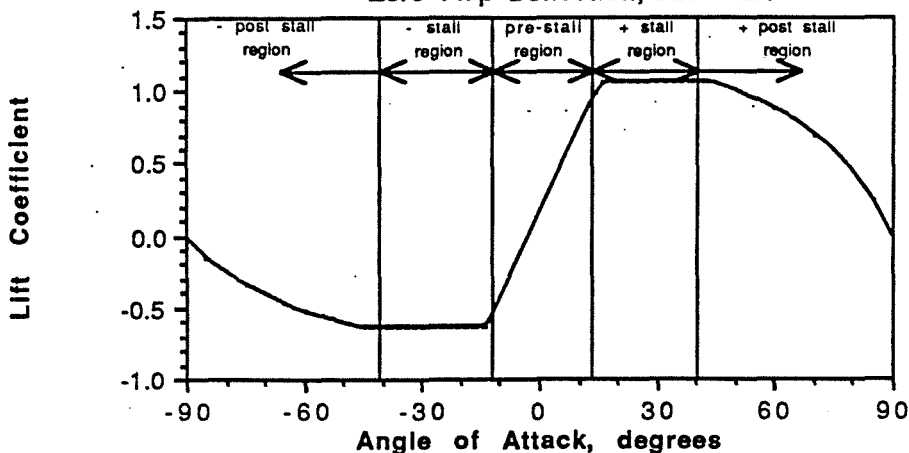
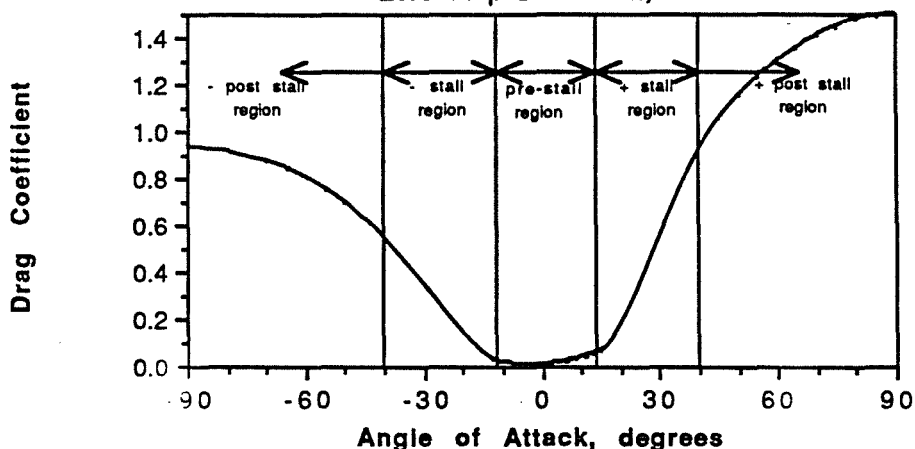


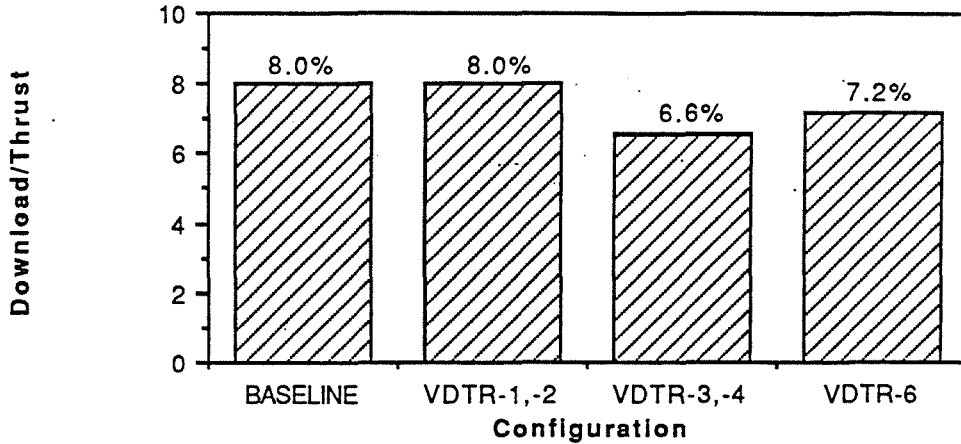
Figure 2 Wing Drag Coefficient Representation  
Zero Flap Deflection, AR = 6.1



### 3.b Vertical Drag and Rotor Performance

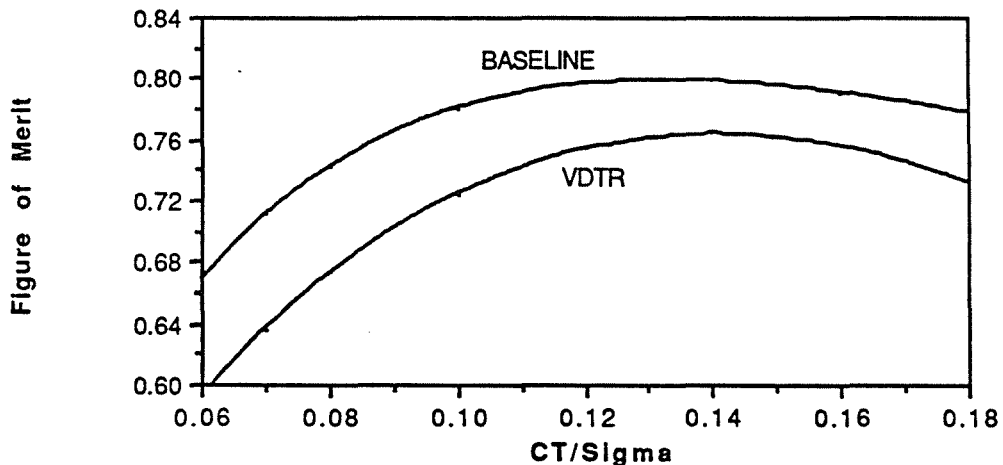
Vertical drag over thrust in hover ( $D_v/T$ ) was estimated using a Prandtl lifting line hover analysis that employs the Biot Savart law to calculate off-blade velocities below the rotor plane. Figure 3 shows the typical variation in vertical drag for the six analyzed designs, with thrust recovery neglected. Note that the high disk loading VDTR designs (nos. 1, 2) have vertical drag equivalent to the conventional tiltrotor, despite a slight increase in wing area outboard of the nacelle. This area is placed in the low downwash zone due to the VDTR spar extension to 42% radius. Reduced download in that zone is offset by increased downwash and download outboard of the 42% spar. Lower downwash velocities associated with low disk loading designs VDTR-3 and VDTR-4 resulted in reduced  $D_v/T$  by 1.4%. The intermeshed, low disk loading VDTR-6 gained 0.6%  $D_v/T$  relative to the VDTR-3 and VDTR-4 due to increased interference from the fuselage and higher downwash velocities where overlap occurs.

Figure 3 Tiltrotor Vertical Drag Variation Predictions



The Baseline tiltrotor and VDTR isolated rotor hover performance is shown in Figure 4. Peak Figure of Merit is approximately equal to 0.8 for the Baseline and 0.76 for the VDTR. As mentioned previously, the VDTR requirement for a large cutout and spar extension result in a .04 degradation of peak Figure of Merit relative to the Baseline. Despite this fact, low disk loading VDTR designs require less power to hover than the Baseline, primarily due to less induced power. The VDTR designs in Table 1 differ in disk loading, solidity, and lateral nacelle spacing which may impose interference variations. However, minor variations in rotor peak Figure of Merit were neglected.

Figure 4 Isolated Rotor Hover Performance at Design Conditions



Steady forward flight rotor power required was predicted for conventional and VDTR tiltrotor designs by an isolated rotor, rigid blade, lifting line, blade element analysis, known as the Generalized Rotor Performance (GRP) code. The real time simulation uses these predictions in a simplified form so that rotor power calculations are included in the real time mechanics. GRP was run for an extensive matrix that defines the tiltrotor envelope, with the specific parameters of rotor advance ratio (or tip speed ratio), thrust, and angle of attack being varied over the expected operating range. The GRP code separates the components of rotor power into induced, profile, H-force and parasite power. This information was used to develop families of curves representing rotor mean drag coefficients and rotor induced efficiencies. Each pass through the (20 Hz) simulation uses an interpolation algorithm to calculate induced and profile power at the specific rotor condition ( $\mu$ ,  $CT/\sigma$ ,  $\alpha$ ). Parasite and

climb power are calculated directly based on rotor attitude, thrust, and flight path horizontal and vertical speeds, respectively.

### 3.c Rotor/Wing Aerodynamic Interaction in Forward Flight

An empirical method was employed which based the variation of download and lift sharing on published V-22 data. This includes the download variation in hover and low speed forward flight, as well as the wing/rotor lift sharing variation throughout the transition from helicopter to airplane mode. Reference 9 supplies the V-22 schedule that was followed in a nondimensional form for hover and low speed download variation. Reference 10 provides the V-22 lift sharing schedule that was modeled over a range of nacelle angles and airspeeds from moderate speed helicopter mode, through conversion and into airplane mode.

### 3.d Twin or Side by Side Rotor Interference Effects

Tiltrotor aircraft operate with twin rotors in a side by side arrangement. Conventional tiltrotors will of course have rotor disks that are separated by some distance greater than the maximum fuselage width. The VDTR aircraft can however have rotor disks that are arranged such that they overlap or intermesh since their capability to retract rotor radius to 66% of the extended radius still allows for a safe rotor blade tip/fuselage clearance. In addition to the advantage of weight savings from reduced wing structure, rotor disks that are laterally adjacent to each other provides a significant benefit from the positive induced interference velocities in low speed helicopter mode flight (Reference 11). Vortex theory indicates that in hover there should be no effect of one rotor upon the other when there is no overlap and the rotors are not vertically separated. This is because in the plane of the rotor but outside the rotor disk, there is no normal induced velocity component and therefore no interference effect. Multi-rotor test data supports this result. In forward flight however, for a single lifting surface the induced velocity is given by wing theory as  $v_{in} = T/(2\rho AV)$  and induced power is proportional to  $(T/\text{span})^2$ . For twin rotors of equal disk area operating at equal thrusts, the total ideal induced power can be represented by  $P = (1+X)P_{\text{isolated}}$  where X is the interference factor for the entire rotor system. It follows that for twin isolated rotors of thrust T and span 2R,  $P = 2(T^2/(2\rho AV))$ . The same two rotors in coaxial arrangement will have total induced power  $P = (2T)^2/(2\rho AV)$  or twice the isolated rotor induced power since the configuration acts like a single rotor with twice the span loading. Thus,  $X = 1$  for coaxial rotors. If the twin rotor configuration with lateral shaft spacing of 2 radii, or disks just touching, is considered, the system acts like a single rotor with the same span loading as the two isolated rotors. Consequently,  $P = T^2/(2\rho AV)$  for the system and  $X = -1/2$ . This favorable interference is the result of each rotor operating in the presence of an upwash from the other rotor. A reduction in the isolated rotor induced power of this magnitude (50%) is realized in theory if the system possesses elliptical spanwise loading. A truly elliptical system loading is not possible for an advancing twin rotor system. Reference 11 indicates past experimental research to show a maximum reduction of induced power of about 35% to be possible when an overlap of approximately 1/4 radius (lateral shaft spacing of 1.75 radii) is present. For rotor disks just touching, data indicates about a 25% reduction in isolated rotor induced power is possible. Figure 5 displays this forward flight information in terms of a factor of isolated rotor induced power as a function of the lateral shaft spacing of the two rotors. Uniform rotor loading is assumed for the coaxial rotor configuration, so that empirical data agrees with theory. Empirical data is extrapolated to determine the lateral shaft spacing of about 2.5 radii where no benefit from twin operation is possible. While lateral shaft spacing for the Baseline tiltrotor is too great (approximately 2.6R) to benefit from this effect, the VDTR makes significant use of this positive interference. A maximum reduction in induced power of 22% is indicated for the VDTR designs with a shaft spacing of 2.05R. A 30% reduction is

indicated for the VDTR-6 with a spacing of 1.93R. Experimental results show that the maximum reduction in induced power occurs at an advance ratio,  $\mu$ , of about 0.09 (35-40 knots) and that the effect is quite small at 100 knots. This is a significant factor in the critical phases of OEI takeoff procedures since low speed climb capability is a crucial factor. Figure 6 shows this benefit for the VDTR-1 design as a function of power required in level flight.

Figure 5 Twin (Side by Side) Rotor Operation in Forward Flight Induced Power Interference Effect

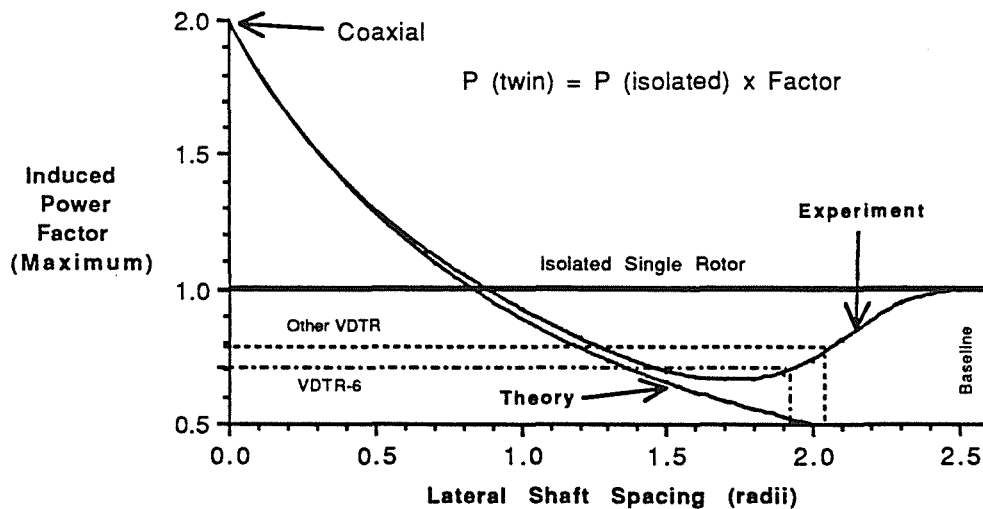
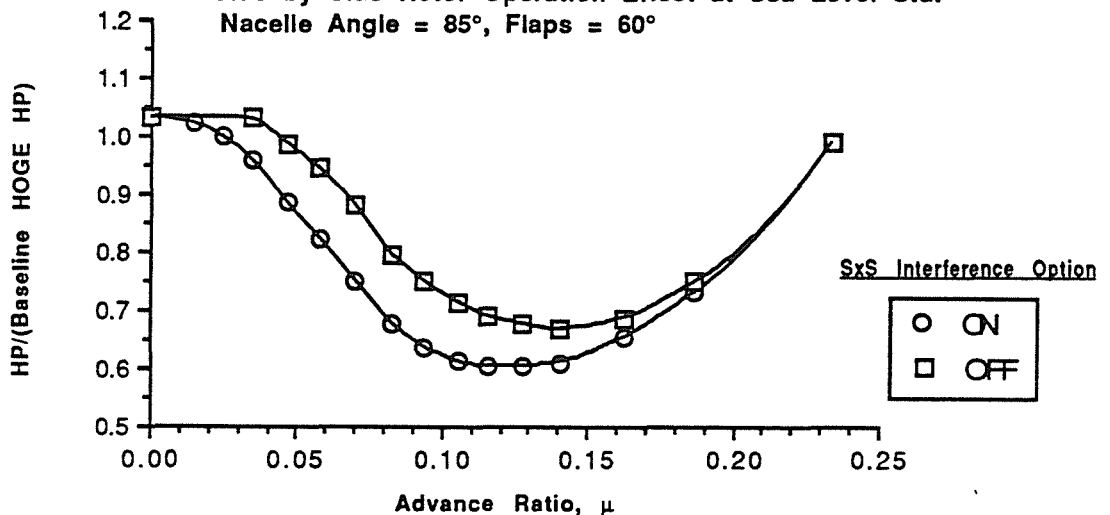


Figure 6 Nondimensional VDTR-1 Power Required versus Advance Ratio Side by Side Rotor Operation Effect at Sea Level Std. Nacelle Angle = 85°, Flaps = 60°



### 3.e Rotor Speed Variation, Rotor Inertia, and Ground Effect

For OEI procedures, it is necessary to model variations in power available due to rotor RPM reduction. This permits substitution of kinetic energy in the rotational system for the deficit of power at a particular condition. This type of modeling is incorporated into the simulation. Estimated values of rotor inertia were used and are nondimensionally tabulated in Table 3.

Table 3 Estimated Rotor Inertias

<u>Configuration</u>	<u>(Rotor Inertia)/(Baseline Rotor Inertia)</u>
Baseline	1.0
VDTR-1	1.26
VDTR-2	1.21
VDTR-3	2.55
VDTR-4	2.45
VDTR-6	2.34

Ground effect was modeled with the use of flight test data. This altered induced power is calculated as a function of rotor height above the ground and horizontal velocity. Currently, only ground level takeoff surfaces are represented. That is, edges of an elevated deck takeoff surfaces cannot be defined.

### 3.f Computer Simulation Architecture

The architecture of the computer simulation has been developed at Sikorsky over a 4 year period. Since it is a custom simulation program, special applications are easily incorporated. Special features added for the tiltrotor simulation were the real time plotting feature and the tiltrotor aircraft graphics model. Current facilities of the simulation include cockpit inside out representation with analog and digital Heads Up Display data displays. Flat, three dimensional digital, or three dimensional contour terrains are available. Data can be saved on preselected parameter and frequency basis with digital printing or plotting post processing facilities. A playback program is also available that can replay a flight profile data file generated from an interactively flown simulation session. The replay simulation can be viewed from any fixed or moving perspective and at any playback speed. The computer image can be directly interfaced to a video recorder. A video tape was made of some of the OEI departures and will be shown during the oral presentation of this paper. The simulation update rate was 20 hertz for the tiltrotor simulation. Hard copies of the video display showing a cockpit and wing man's view of the simulation display are shown in Figures 7 and 8.

91 - 26.11

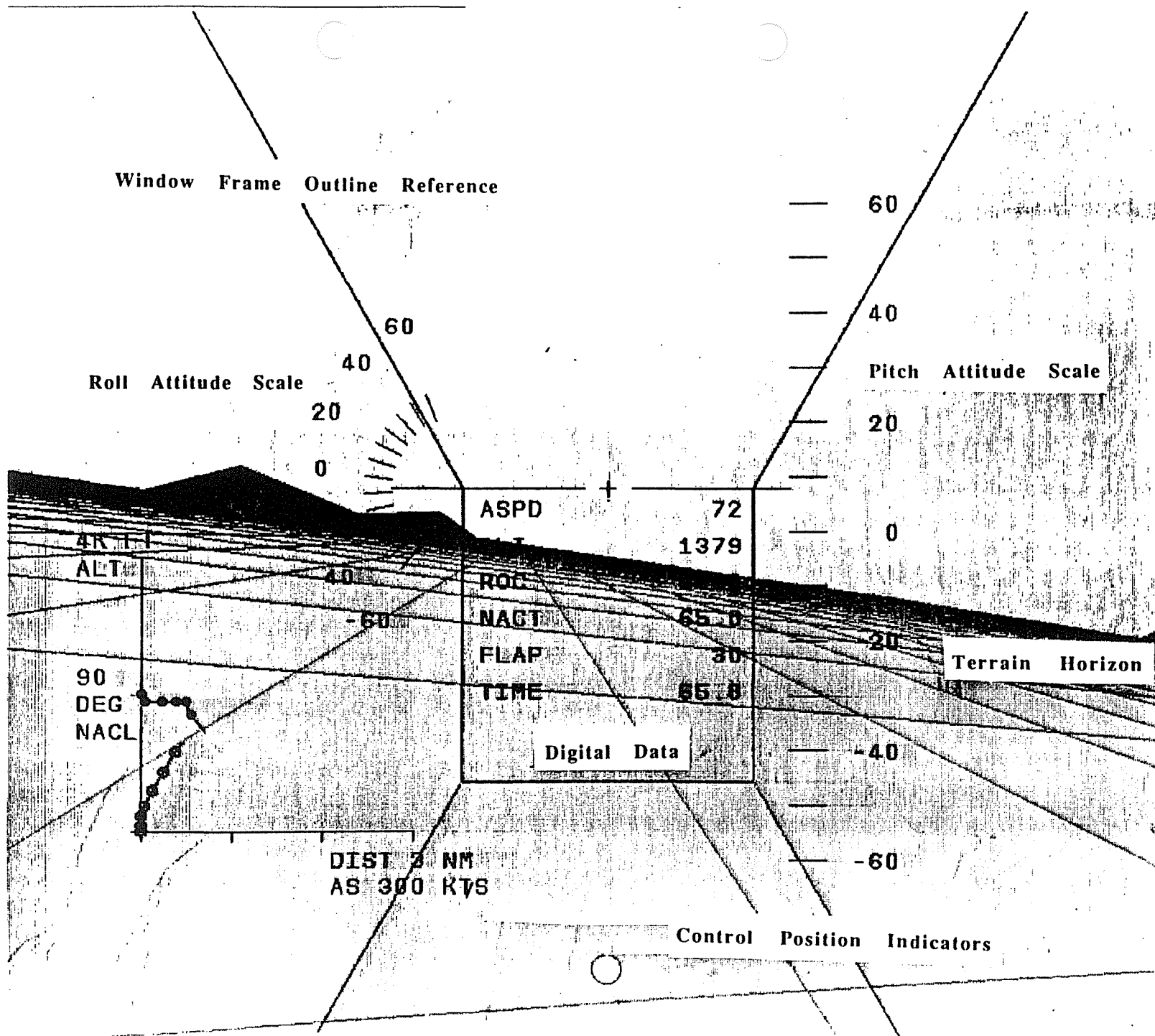


Figure 7 View From Cockpit of Tilt Rotor With Heads Up Display

91 - 26.12

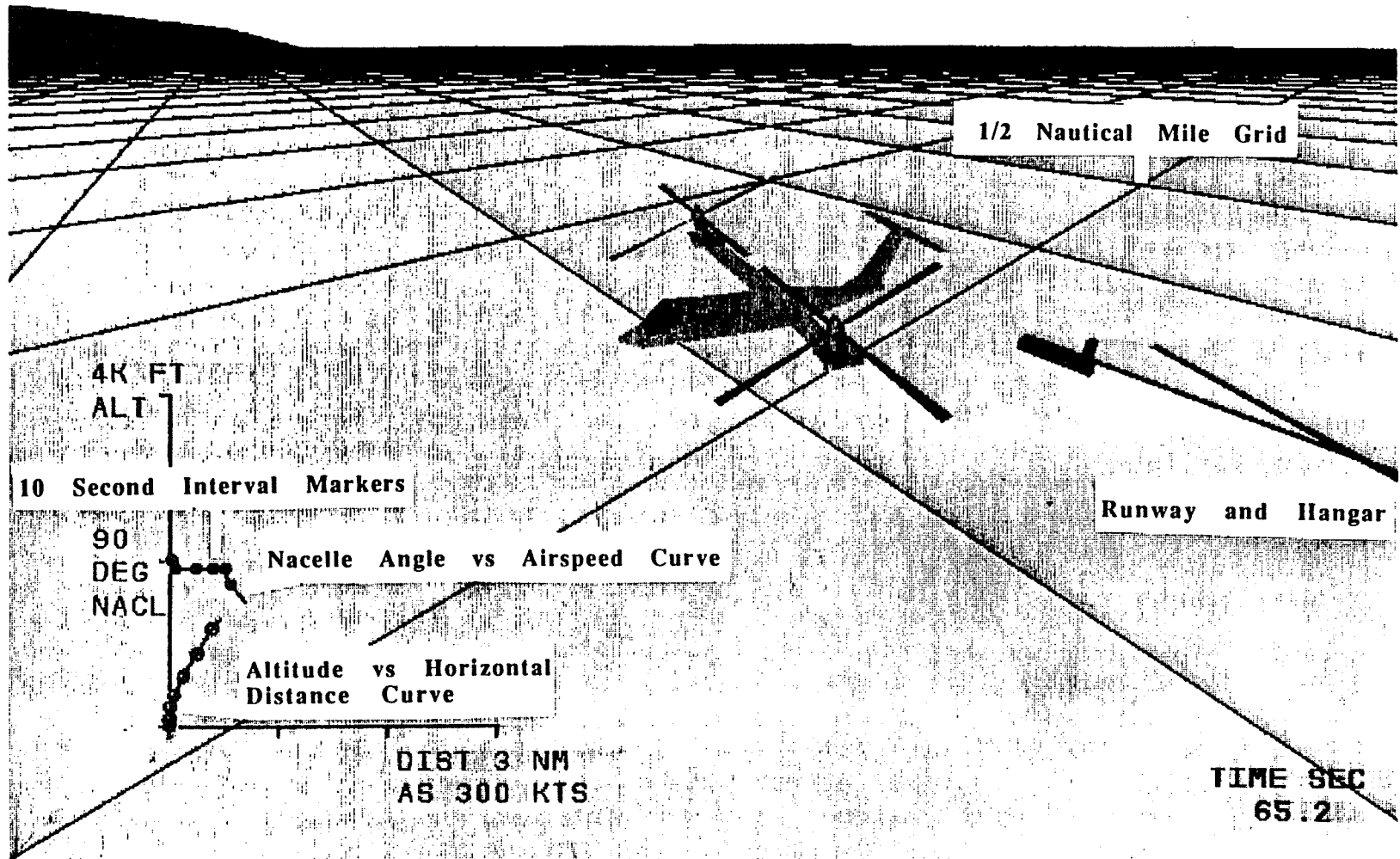


Figure 8 Wingman View of Computer Simulation Scene

#### 4. Simulation Results - Level Flight Performance and Climb Capability

Nondimensionalized level flight power required polars generated by the simulation in helicopter mode are given in Figures 9 for the Baseline, VDTR-1 and VDTR-3 (fixed engine design), and in Figure 10 for the VDTR-2, VDTR-4, and VDTR-6 (rubber engine designs). These predictions are at sea level standard with a nacelle angle,  $\sigma = 85^\circ$ , and a flap angle of  $60^\circ$ .

Figure 9 Nondimensional Power Required versus Advance Ratio  
Baseline Engine Designs at Sea Level Standard  
Nacelle tilt =  $85^\circ$ , Flap angle =  $60^\circ$

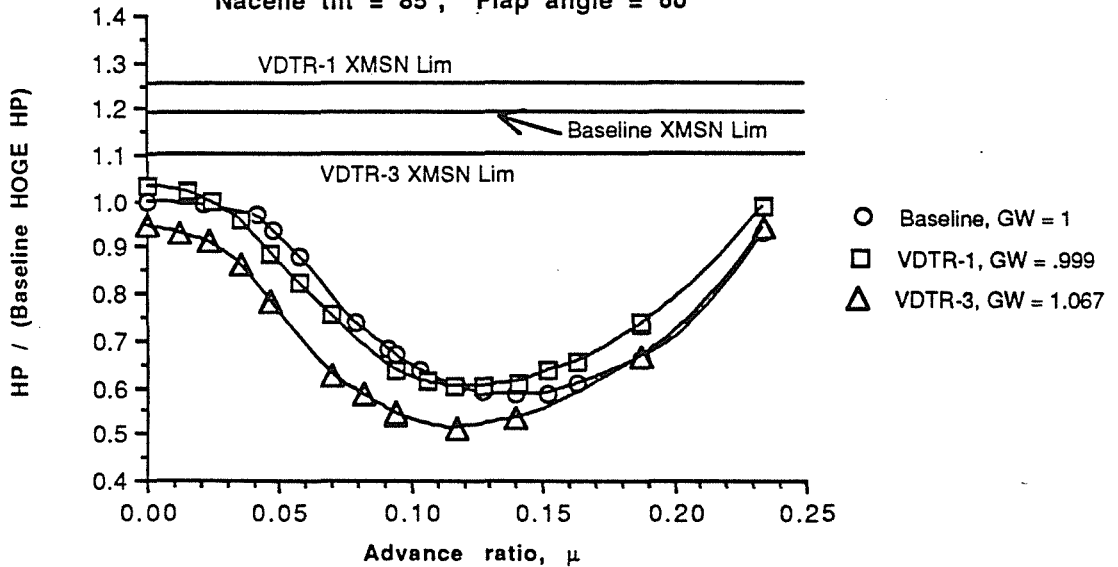
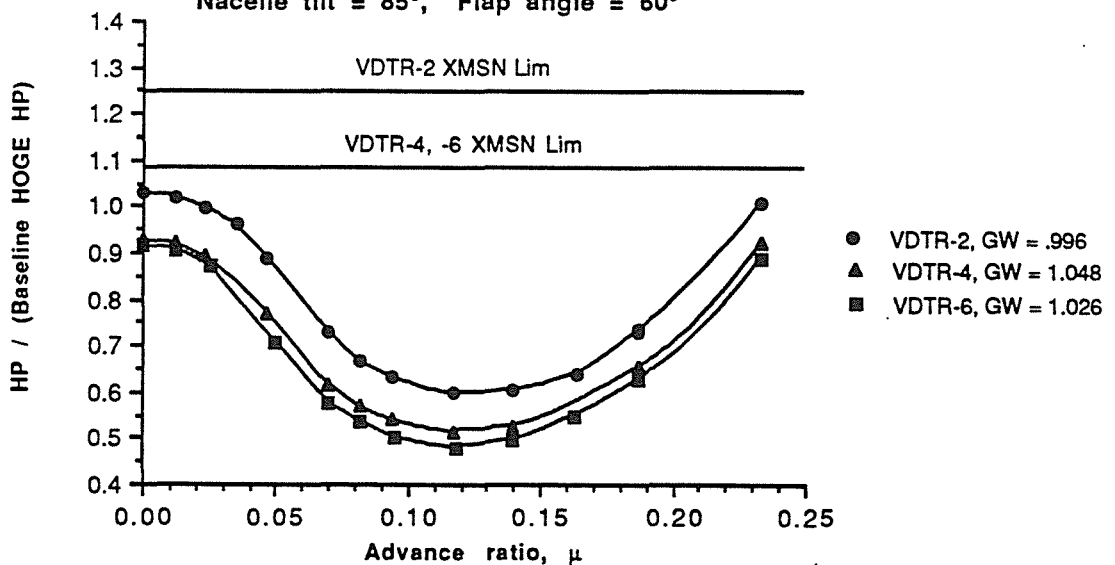


Figure 10 Nondimensional Power Required versus Advance Ratio  
VDTR Rubber Engine Designs at Sea Level Standard  
Nacelle tilt =  $85^\circ$ , Flap angle =  $60^\circ$



Notice that minimum power airspeed varies slightly between the configurations. The Baseline minimum power advance ratio,  $\mu$ , is about 0.14 (60 knots). The VDTR-1 and VDTR-2

(high disk loading) designs reach minimum power required near  $\mu = 0.128$  (55 knots) while the VDTR-3, VDTR-4, and VDTR-6 (low disk loading) designs reach minimum power required near  $\mu = 0.117$  (50 knots). The lower minimum power airspeed of the VDTR designs is due to the beneficial side by side rotor interference discussed previously. Since this effect is greatest at about  $\mu = 0.09$ , but drops off fairly rapidly thereafter, it will act to enlarge the low speed end of the VDTR power required bucket. The low disk loading of the VDTR-3, VDTR-4, and VDTR-6 acts to further reduce minimum power airspeeds.

Table 4 presents the ratio of minimum power to HOGE power for these aircraft at the design condition. Notice that for all of the VDTR designs this ratio is smaller than it is for the Baseline. Since the VDTR-1 and VDTR-2 are identical in disk loading to the Baseline, this small difference is due to the side by side rotor interference and slightly increased wing areas and subsequent lift. The VDTR-3 and VDTR-4 have even lower ratios of minimum power to HOGE power due to slightly more benefit from side by side rotor interference (nacelle shaft spacing is 2.044R for the VDTR-3,-4 compared to 2.054R for the VDTR-1,-2) and again more wing lift than relative to the Baseline. The additional wing lift for the three low disk loading VDTR designs is the result of significant wing area increases, and higher wing angles of attack from lower rotor induced velocities on the wing. The ratio of minimum power to HOGE power is lowest for the VDTR-6 because of the overlapped rotor design (shaft spacing of 1.93R).

**Table 4 Minimum/HOGE Power & Climb Rate Capability**  
Nacelle Tilt = 85°, Flaps = 60°, Design Condition

<u>Configuration</u>	<u>Min HP/HOGE HP</u>	<u>HP Available/Baseline HPav</u>	<u>Maximum Rate of Climb(fpm)</u>
Baseline	.605	1.0	1842
VDTR-1	.585	1.116	2406
VDTR-2	.580	1.111	2470
VDTR-3	.553	1.008	2135
VDTR-4	.552	0.987	2162
VDTR-6	.522	1.049	2275

Nondimensional power margin available for climb and climb rate capability, predicted by the simulator at the minimum power airspeeds, are also presented in Table 4 for helicopter mode operation. It is noted that all VDTR designs have significantly better helicopter mode climb rate capability than the 1842 fpm of the Baseline. The VDTR-1 and VDTR-2 have the highest maximum climb rates (about 2430 fpm); the VDTR-3 and VDTR-4 maximum climb rates are about 2150 fpm, and the VDTR-6 maximum climb rate is about 2275 fpm. Variations are due primarily to the combination of the transmission sizing procedure, side by side rotor operation, disk loading effect, and the variation in wing area among the various designs. Recall that transmissions are sized by 115% of the HOGE power at the design takeoff condition. Since the VDTR-1 and VDTR-2 have the same disk loading as the Baseline and compromised rotor hover performance, they therefore have higher HOGE powers than the Baseline. Consequently, higher transmission ratings of the VDTR-1 and VDTR-2 combined with their lower ratios of minimum power to HOGE power than the Baseline, result in a significant gain in power available to climb. For the VDTR-3, VDTR-4, and VDTR-6 even though rotor hover Figure of Merit is not as good as the Baseline, the larger radius associated with their low disk loading results in a lower thrust coefficient and significantly less induced power. This yields a hover power that is less than the Baseline even though they have increased gross weights. Again, the transmissions were sized by approximately 115% of (a now lower than the Baseline) HOGE power, but counteracting this is even lower minimum

power to HOGE power ratios, so that power available to climb is approximately the same for the VDTR-3 and VDTR-4 as it is for the Baseline. The main reason that these designs have greater maximum climb rates than the Baseline is because they have significantly lower minimum power airspeeds, resulting in less of a profile power increase than the Baseline as the rotor thrust is increased to climb. Available climb power for the VDTR-6 is slightly greater than it is for the Baseline due mainly to the rotor overlap effect. The VDTR-6 also does not encounter as much of a profile power penalty in climb as the Baseline. Another advantage realized by the VDTR in climb comes from reduced rotor tip speed ratios that result from a cosine effect on rotor angle of attack in climb. Reducing the tip speed ratio,  $\mu$ , yields an increase in benefit from side by side rotor interference, since this effect is modelled to be at a maximum at tip speed ratios lower than the minimum power tip speed ratio.

Climb capability in airplane mode was not examined, although it is important to the mission. The VDTR RPM is reduced in airplane mode by only 5% to obtain a higher cruise efficiency, so the transmission rating is reduced by 5% also. This affords the VDTR designs a significant increment of power available for airplane mode climb that the Baseline does not possess. The Baseline requires an RPM reduction of 20% to gain higher propeller efficiency, which reduces the transmission rating by 20%. The climb advantage enjoyed by the VDTR both in helicopter mode and especially in airplane mode might make it desirable to size the various VDTR transmissions by less than the current 115% of HOGE power, in order to reduce the gross weight. The weight savings realized from a smaller transmission should not have a large effect on Category A vertical takeoff capability since the effect of each one separately tends to offset the other. That is, less gross weight results in more OEI climb power available for a given engine and thus improved Category A performance. A smaller transmission reduces the initial vertical climb rate through CDP (as described in the next section), thus reducing kinetic and potential energy necessary for continued takeoff procedures and therefore reduces Category A vertical takeoff capability. A sensitivity study is recommended to establish a relation between transmission weight savings and Category A performance. However, it is estimated that a reduction in VDTR transmission sizes by approximately 3% would save about 100 pounds and not have a significant effect on Category A performance.

## 5. Simulation Results - Category A Vertical Takeoff Procedure

### 5.a General Description

Category A takeoff procedures are those that are used on multi-engine aircraft to minimize risk involved if one engine becomes inoperative during takeoff. The Critical Decision Point (CDP) as used here is that point in the takeoff flight path at which an engine can fail and the vertical height will permit a rejected takeoff (RTO) or a continued takeoff (CTO). If an engine should fail prior to the CDP, the takeoff must be rejected. A maximum allowable touchdown speed of 400 feet per minute was assumed for rejected takeoffs. If an engine should fail at or after the CDP, the aircraft is then accelerated to  $V_{TOSS}$  (TakeOff Safety Speed).  $V_{TOSS}$  is that airspeed which will produce a steady rate-of-climb, out of ground effect, in accordance with the climb criteria published in Reference 12. The specific procedure used to determine the CDP is described later. Figure 11 displays a typical one engine inoperative (OEI) continued vertical takeoff profile initiated from a ground level heliport pad. A dynamic procedure is represented by Segment 1. During this segment, a minimum height along the flight path (or ground clearance) is reached. This minimum height requirement is assumed to be 35 feet for ground level takeoffs, so that consistency is maintained with Category A helicopter operation. OEI 30 second power is available from the point of engine failure, but cannot be used to satisfy climb segment requirements. Segment 1 is terminated once  $V_{TOSS}$  is achieved and steady rates of climb can be maintained. Segments 2 and 3 are steady climb

segments that use maximum continuous power (MCP) ratings. The climb criteria is described in more detail below.

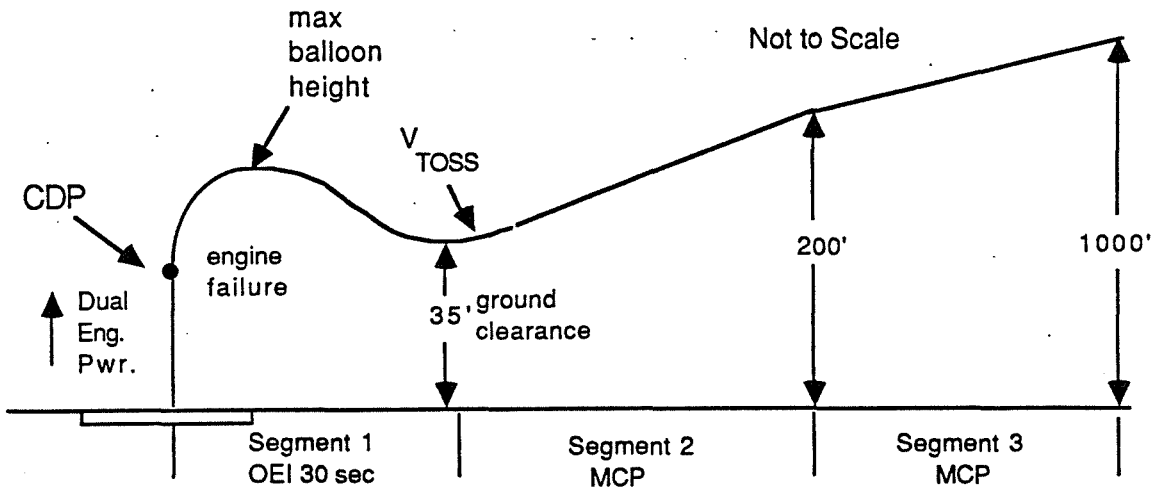


Figure 11 Ground Level Category A OEI Vertical Take-off Profile

Figure 12 displays a similar vertical procedure for elevated helideck takeoffs. The primary difference between this and the ground level procedure is that the minimum height requirement is assumed to be 0 feet with respect to the helideck level. A clearance radius of 15 feet from the edge the deck is also typically required.

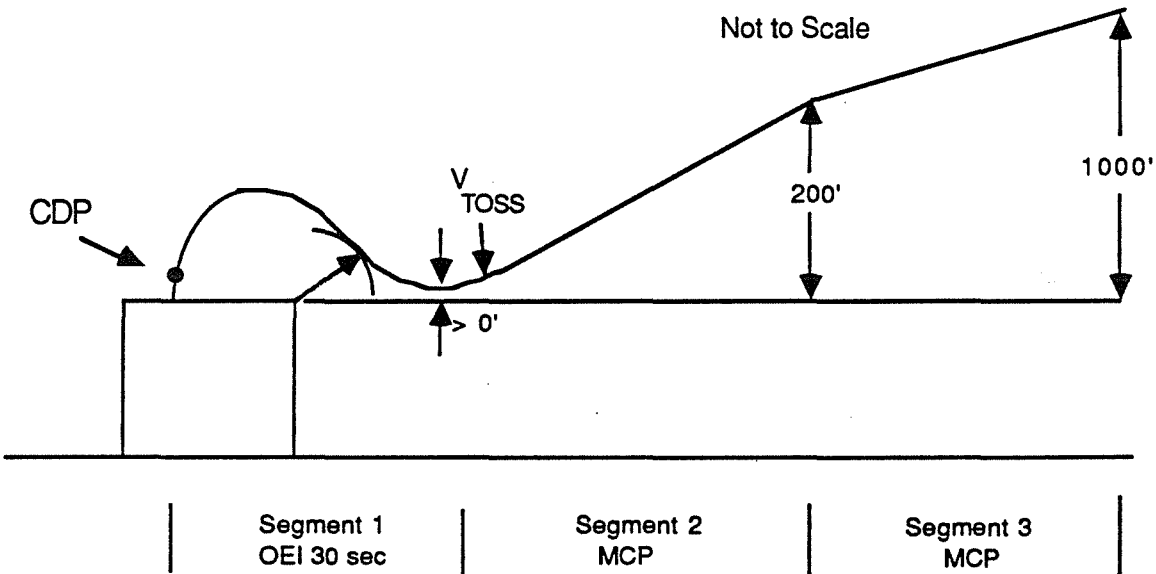


Figure 12 Elevated Deck Category A OEI Vertical Take-off Profile

### 5.b Climb Criteria

As the tiltrotor represents a hybrid category of aircraft, the U. S. Federal Aviation Administration (FAA) considers them to be sufficiently unique to require new criteria. Consequently, Reference 12 was published to define and supply an interim criteria. For a two-engine tiltrotor aircraft vertical takeoff procedure, these criteria are interpreted as:

1. From the height between the end of the dynamic segment of the vertical procedure and 200 feet above the takeoff surface, using OEI maximum continuous power (MCP), a steady climb without ground effect must not be less than the greater of a 2.4 percent gradient or 200 feet per minute.
2. From 200 feet through 1000 feet above the takeoff surface, using OEI maximum continuous power (MCP), the steady gradient of climb must not be less than 1.2 percent.

For the various configurations simulated,  $V_{TOSS}$  was generally between 30 knots ( $\mu = .07$ ) and 40 knots ( $\mu = .09$ ). Best rates of climb are realized at higher airspeeds as can be seen in the level flight performance section, Figures 9 and 10.

### 5.c Critical Decision Point Determination - Continued Takeoff Procedure and Results

At specific operating conditions and with ground effect included, the simulated OEI Category A vertical takeoff procedure consisted of an initial vertical climb at dual engine maximum transmission power up to a predetermined wheel height, where an engine failure would occur. The continued takeoff (CTO) procedure then included an initiation of horizontal speed (via nacelle tilt) accompanied by a reduction in rotor collective pitch, thus reducing power usage to the OEI 30 second rating. For the period when more power is required to maintain a condition than is available, a reduction in rotor speed occurs, determined as a function of rotor inertia and the power deficit. Maximum RPM reductions of 12-13% were considered acceptable. For the higher inertia VDTR rotor systems, a noticeably slower spooling down of RPM was possible relative to the Baseline, thus maximizing ballooning (vertical ascent after engine failure) and ground clearance. As the low disk loading VDTR rotors have nearly twice as much inertia as the high disk loading VDTR designs, this was even more of a factor for those designs. As mentioned, nacelle tilt was used to initiate forward speed. This was performed automatically at the rate of 3°/sec to some final nacelle angle. It was found that ending nacelle angles of 70° - 80° allowed for rapid enough accelerations to  $V_{TOSS}$  and yielded increased benefit from wing contributions as airspeed is increased. This was also found to reduce pilot workload, since minimal body pitch adjustments through cyclic pitch inputs were required until speeds of about 20 knots were achieved, when a nose up attitude would be required to maximize the ground clearance along the flight path by increasing wing lift and rotor lift amounts. When engine failure heights were below 25 feet, nacelle angles of 80° were used for the climb-out combined with body attitude of about 5° - 10°. For engine failure heights above 25 feet, nacelle angles of 70° with body attitudes approaching 15° were used for the climb-out segments.

For each predetermined engine failure height that was flown with the simulation at a particular atmospheric condition and gross weight, the minimum height along the flight path was recorded. Figure 13 displays a plot of this parameter as a function of engine failure height for the Baseline and the VDTR designs at the design condition at each configuration's

design gross weight and with ground effect being included. Each curve intersects the ground level takeoff requirement height of 35 feet at a point that corresponds to the minimum CDP height for that condition. For the configurations considered, this minimum CDP height ranges from about 10 feet for the VDTR-4 to about 20 feet for the Baseline and VDTR-2. This procedure can be repeated using the dashed line on Figure 13 representing the elevated takeoff surface minimum height requirement (0 feet). For the configurations shown, minimum CDP heights are very close to zero for elevated deck takeoffs. As long as safe rejected takeoffs can be accomplished at higher heights, it is likely that the procedure would be developed for a CDP greater than 10 feet. Note that the VDTR-3 and VDTR-6 are sufficiently powered such that a continuous climb can be maintained after an engine failure at this condition, even as horizontal acceleration occurs. Figure 13 includes ground effect. Figure 14 quantifies the effect of the ground on these vertical takeoff procedures for the Baseline configuration. As expected less effect from the ground is evident as engine failure height is increased. Ground effect acts to increase initial vertical rates of climb (maximizing balloon height) and also slightly affects power requirements when the aircraft descends to nearly ground level during the acceleration to  $V_{TOSS}$ . Since ground effect is essentially negligible at speeds above 30 knots with wheels very close to the ground, the inclusion of this latter effect of the ground should not significantly impact the results in Figure 13 for elevated deck operation (for which the ground effect model does not recognize).

**Figure 13 Comparison of Critical Decision Point Heights for OEI Continued Vertical T-O Procedures (IGE) Ground Level & Elevated Deck @ Design Condition**

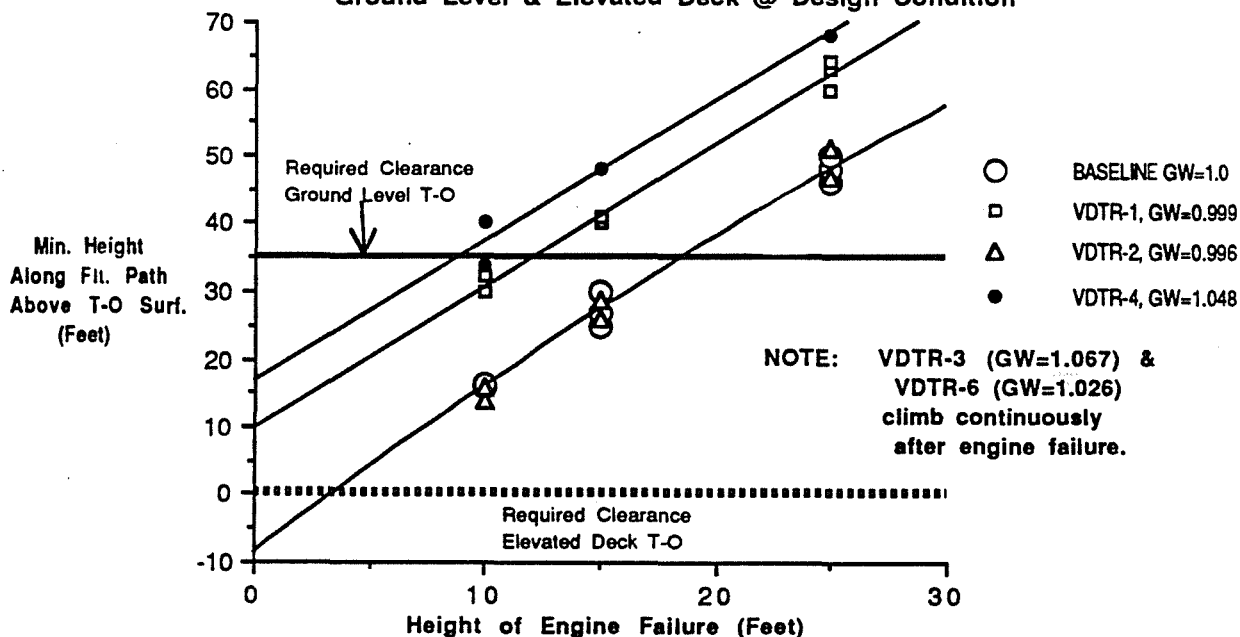
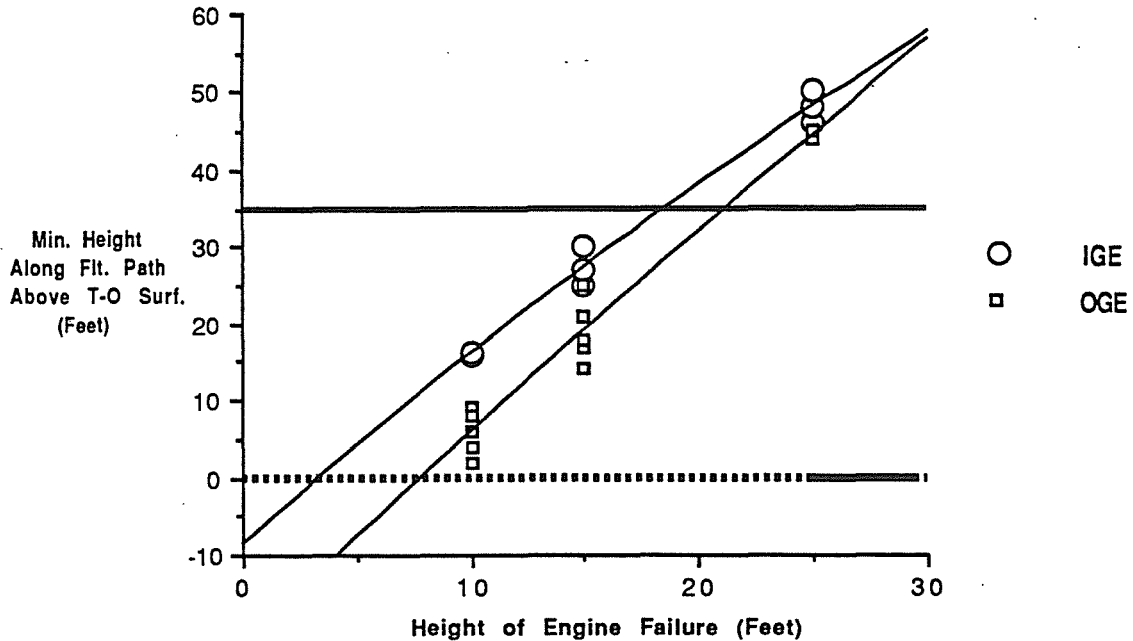


Figure 14 Predicted Baseline OEI CTO Procedures  
CDP Determination @ Design Condition



5.d Critical Decision Point Determination - Rejected Takeoff Procedure and Results

To determine the maximum CDP that can be used for each configuration at a particular condition and gross weight, a maximum and/or reasonable engine failure height must be found whereby a rejected takeoff can successfully be performed. The procedure as flown on the simulation once again (including ground effect) begins with a vertical climb with dual engine power at the transmission rating. An engine failure occurs at some designated height. In order to minimize the ballooning height, or the extra height gained after engine failure due to climb momentum, and also to minimize rotor RPM droop, the pilot will lower collective blade pitch until the power level is well below the OEI 30 second power. Once 100% rotor speed is restored and a descent rate is achieved, OEI 30 second power is used to minimize this descent rate until approximately 20 - 30 feet above the landing surface. At this time, collective pitch is increased (as much as 5°/sec was used), substituting rotor kinetic energy for the demand for power so that touchdown speed is reduced. Rotor RPM reduction to 78% was permitted for rejected takeoffs with touchdown speeds of 400 ft/min.

For the design condition GW, successful rejected takeoffs were accomplished with the simulation at engine failure heights of 100 feet for all configurations. While this may be possible in an analytic sense, certain factors must be considered along with this information. Such factors include wind speed, helipad size, cockpit visibility (pilot cues) and also the possibility of entering the vortex ring state in descent. These realisms that affect the ability to land back to the same location are not modelled in the simulation. Therefore, maximum CDP for a rejected takeoff was assumed to be 50 feet.

5.e Payload Capability Based on Category A Requirements

Figure 15 shows all of the Baseline and VDTR CDP determination runs (each point represents a run) used to determine the payload for each configuration as a function of altitude at an ISA +10°C atmosphere. This figure demonstrates that by varying gross weight for each configuration, a consistent CDP height was maintained, which did not exceed a maximum of 50 feet for ground level operation, and Category A CTO requirements were satisfied. The resulting gross weight then determined the payload capability as a function of altitude with ISA + 10°C, shown in Figure 16. Rejected takeoff capability is satisfactory for all cases analyzed. It is noted that for elevated deck operation the payload capability in Figure 16 corresponds to a CDP of approximately 25 feet. Obviously, as CDP height goes up, so too does the payload. Thus, payload predictions may be slightly pessimistic if elevated deck operation is performed and CDP height is preferred to be greater than 25 feet. It is clear from Figure 16 that the low disk loading VDTR designs have a significant payload advantage at high altitudes. The VDTR-3 is shown to have as much as a 2200 pound (or 11 passengers) payload advantage at an altitude of approximately 1750 meters (5700 ft.) with ISA + 10°C. This type of benefit would of course be similar at even higher temperatures. It is worth noting that maximum payload is assumed to be approximately 6000 pounds in Figure 16, based on a 30 passenger mission. If the structural specifications permit payloads greater than this and if other missions are defined (more passengers, cargo, and/or military options) that require greater payloads, then the maximum payload advantage of the VDTR-3 would be realized at lower altitudes as well. The VDTR-6 is noted to be next best with respect to payload capability at high altitudes. Relative to the Baseline, the VDTR-6 payload advantage is approximately 1400 pounds, or 7 passengers at an altitude of approximately 1380 meters (4500 ft).

**Figure 15 Category A Vertical Takeoff Procedure  
Minimum Height Variation vs. CDP Height  
For Payload Capability Determination  
All Configurations, GWs, Altitudes**

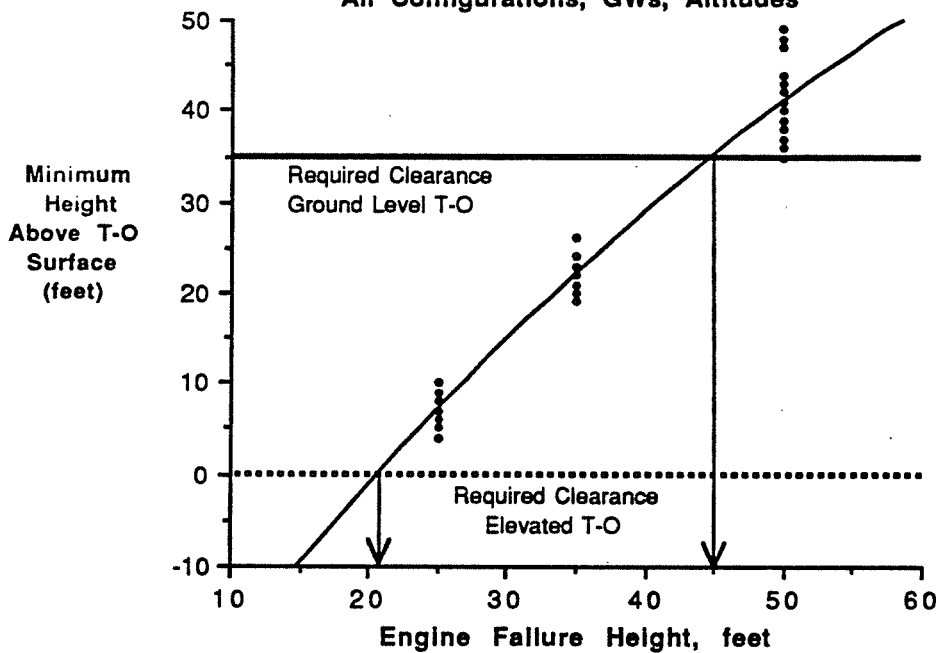
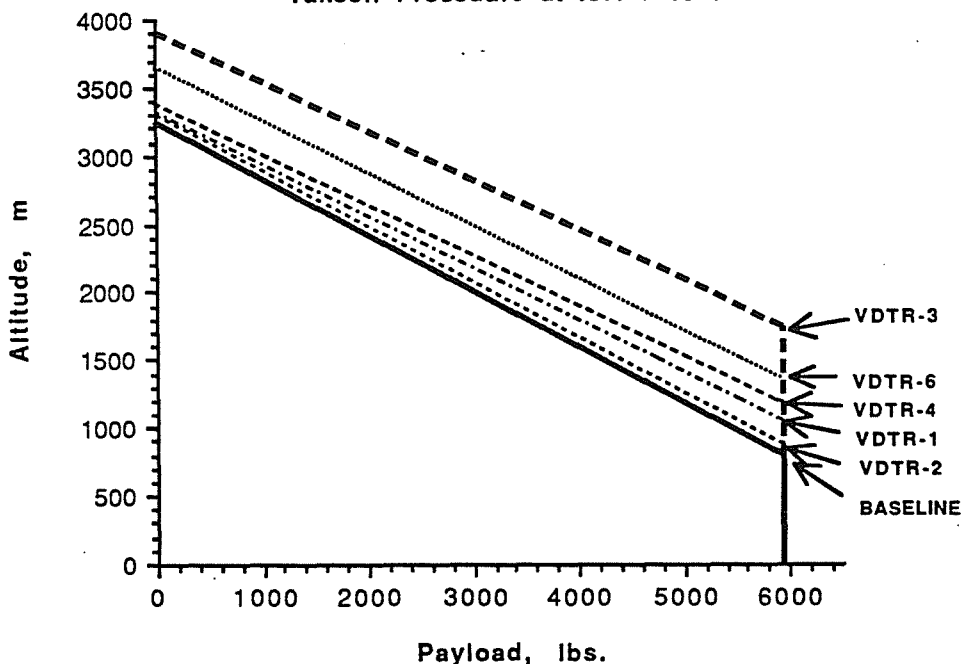


Figure 16 Payload Capability vs. Pressure Altitude  
Based on Category A OEI Vertical  
Takeoff Procedure at ISA + 10°C



## 6. Conclusions

A real time tiltrotor simulation program has been developed and used to predict tiltrotor level flight performance, helicopter mode climb capability, Category A vertical takeoff performance. Rotor system design features have a significant effect on the flight performance. The variable diameter tiltrotor (VDTR) option provides an opportunity to obtain the following benefits relative to the Baseline conventional tiltrotor:

1. Low disk loading VDTR designs (-3, -4, & -6) have lower rotor downwash velocities resulting in less vertical drag in hover and higher wing lift in helicopter mode forward flight from less wing interference.
2. All VDTR designs receive benefit from twin or side by side rotor interference, which has the effect of significantly reducing induced power requirements in low speed helicopter mode flight. This benefit is a dominant factor in the Category A takeoff performance of the VDTR designs, and also affects VDTR climb rate capability in helicopter mode.
3. The low disk loading VDTR designs (-3, -4, & -6) provide significantly improved Category A vertical takeoff performance which improves safety margins at the design conditions and enhances payload capability at altitudes and temperatures above the design condition. Primary characteristics responsible for this include the beneficial side by side rotor interference, increased rotor system inertia, increased wing area, and the low disk loading effects of less vertical drag, less wing interference near minimum power airspeed, and lower minimum power airspeeds.

4. All VDTR designs provide improved helicopter mode climb rate capability of at least 15%. VDTR climb rate capability in airplane mode should be improved by much more. This is due to additional power available to climb that results from less of a RPM reduction and corresponding transmission rating reduction than the Baseline undergoes in airplane mode. This excess of climb capability for the VDTR exposes an opportunity to save weight by reducing transmission sizes.
5. All VDTR designs should have better powerplant performance that comes about with reduced requirements for RPM variations.
6. The VDTR-4 and VDTR-6 designs offer the benefits of a significantly reduced engine size and better balance of power. This translates to advantages manifested in reductions of: engine dry mass, investment costs, maintenance costs, fuel consumption, and aerodynamic drag.
7. VDTR designs should have reduced acoustic footprints that result from improved climb rate capability in both helicopter mode and airplane mode. Reduced minimum power airspeeds will allow even steeper climb gradients, further minimizing acoustic footprints. Additionally, VDTR designs should have significantly less cabin noise levels since airplane mode tip speeds are lower and VDTR designs without rotor overlap have greater tip/fuselage clearance than the Baseline. Only the VDTR-6 has less tip/fuselage clearance than the Baseline.

The attractive benefits of the VDTR designs mentioned above need to be traded off against the negative aspects of each particular VDTR design before any tiltrotor variation can be declared the best for the particular mission under consideration. The VDTR disadvantages consist of but are not necessarily limited to rotor system investment and maintenance costs, reduced rotor Figure of Merit and increased gross weight.

The authors would like to acknowledge the contributions of various individuals: Andy Vadasz for his assistance with OEI takeoff procedures, Mark Scott for his preliminary design efforts, S. Jon Davis for his aerodynamic design analyses, Evan Fradenburgh and Bob Moffitt for their always insightful comments and guidance, and also helpful discussions with Dave Matuska and Joe Visintainer.

## 7. List of References

1. Boeing Commercial Airplane Group and Helicopters, Bell Helicopter Textron, Inc., "Civil Tiltrotor Missions and Applications, Phase II: The Commercial Passenger Market", NASA CR 177576, February 1991.
2. Caramaschi, V., "The EUROFAR Vehicle Overview", American Helicopter Society Annual Forum, May, 1991.
3. Fradenburgh, E. A. "Improving Tilt Rotor Aircraft Performance with Variable-Diameter Rotors", Fourteenth European Rotorcraft Forum, Paper no. 30, September, 1988.
4. Dabundo, C. and Kimball, D., "Initial Flight Test Assessments of V-22 Flying Qualities", American Helicopter Society Annual Forum, May, 1990.
5. Muggli, W., "Engine Aspects in the Design of Advanced Rotorcraft", Fourteenth European Rotorcraft Forum, Paper no. 24, September, 1988.
6. Jacobs, E., Pinkerton, R., and Greenberg, H., "Tests of Related Forward-Camber Airfoils in the Variable-Density Wind Tunnel", U.S. National Advisory Committee for Aeronautics, Report No. 610, Washington, D.C., 1937.
7. Ramm, H., Schlichting, H., and Truckenbrodt, E., Aerodynamics of the Airplane, McGraw-Hill International Book Company, 1979.
8. Hoerner, Sighard F., Fluid Dynamic Drag, Great Britain, 1958.
9. McVeigh, M.A., Grauer, W.K., and Paisley, D.J., "Rotor/Airframe Interactions on Tiltrotor Aircraft", American Helicopter Society Annual Forum, June, 1988.
10. Dunford, P., Lunn, K., Magnuson, R., and Marr, R. "The V-22 Osprey - A Significant Flight Test Challenge", Sixteenth European Rotorcraft Forum, Paper no. II.7.3-1, September, 1990.
11. Johnson, Wayne, Helicopter Theory, Princeton University Press, Princeton New Jersey, 1980.
12. U. S. Department of Transportation, Federal Aviation Administration, "Interim Airworthiness Criteria Powered-Lift Transport Category Aircraft", Southwest Region, Fort Worth, Texas, July, 1988.